*Science of Sintering*, **55** (2023) 189-203

https://doi.org/10.2298/SOS220828005L

UDK: 625.074; 620.181.4

# Oxide Powder Mixture with Poly-vinyl Alcohol (PVA) and added Polyethylene Glycol (PEG) as Plasticizer

**Nebojša Labus[1*)], Jugoslav Krstić[2], Srdjan Matijašević[3], Vladimir Pavlović[4]**

[1]Institute of Technical Sciences of the Serbian Academy of Sciences and Arts, Knez Mihailova 35/IV, Belgrade, Serbia

[2]University of Belgrade – Institute of Chemistry, Technology and Metallurgy, Njegoševa 12, 11000 Belgrade

[3]Institute for Technology of Nuclear and Other Mineral Raw Materials (ITNMS), 86 Franchet d Esperey St., 11000 Belgrade, Serbia

[4]University of Belgrade - Faculty of Agriculture, Nemanjina 6, Belgrade – Zemun, Serbia

***Abstract:***

*Powder mixture consisted of ZnO, $Mn_2O_3$ ($MnCO_3$) and $Fe_2O_3$ blended powders, was found laminating during compaction. Polyvinyl alcohol (PVA) and a combination of PVA with polyethylene glycol (PEG) added as a plasticizer, were introduced as polymer binders to improve the compaction of oxide mixtures. It has been done by forming a suspension of oxide mixture and varying the polymer solution concentration and composition. By evaporating the solvent, new materials were obtained, which consist of oxide particles bound via polymer. In such a manner obtained hybrid materials were characterized with attenuated total reflection Fourier transformed infrared (ATR-FTIR) spectroscopy, differential thermal analysis (DTA) and transmission electron microscopy (TEM). The oxide polymer material was compacted at 200 MPa and the expansion of this compact during heating was monitored in temperature range up to 550ºC with dilatometer. It was found that PVA forms graft polymer with PEG and specific interaction with oxide particles surface was revealed.*

***Keywords**: Oxide nano powders, Compaction, Thermal properties, PVA binder.*

## 1. Introduction

Compaction of the homogenized but morphologically different powders in a mixture is engaging variety of powder particle shapes and dimensions that should form contacts during packing. When these powders are as well chemically different, contacts engage different friction between powder particles and system has one more variable [1]. This leads to a non-uniform distribution of the nominal forces transmitted from the tool through the compact. Nano dimensional oxide powder [2] possesses individual particulate brittleness, but during compaction an ordered network forms by attached particles and elasticity of the compacted specimen is emerging [3]. Thus, even when the lowest pressures for powder compaction were applied, after the pressure removal, elasticity of the assembly consisted of powder particles induces lamination of the compact [4]. Using binder in a process of the

*) **Corresponding author:** nebojsa.labus@itn.sanu.ac.rs

powder compaction, brings numerous subside impeding phenomena during the subsequent sintering process. Alternatively, good compaction ability can be achieved as well with prior mechanical milling of the powder, but in that case the powder`s size and morphology are inevitably lost [5].

Binders are often polymers that should wrap on the metal oxide powder particle`s surface enabling firm contact between powder particles. Polymers are usually encountered as solids, either in amorphous or crystalline state, able to form a solution with liquid solvents. Oxide powder forms a suspension with a solution of diluted polymer, which then can be sprayed using aerosol-assisted self-assembly technique combined with drying. This method produces newly formed particles consisted of bound powder particles. These new particles are spherical in shape, larger, have a relatively monodispersed size, they are mutually agglomeration-free, bringing very useful properties regarding further material processing. This evaporation process is known as spray drying technique [6]. Anyway, conventional thermal evaporation of solvent, as well, brings oxide particles to bind together using polymer.

A polymer in a solution has a secondary structure, conformation, depending on the interaction polymer - solvent. Chains can be fully solvated and relatively extended, and then polymer molecules are randomly coiled. A measure of the size that polymer molecule occupies in a solution is defined with the radius of gyration value. Radius of gyration is average distance of the mass of the molecule from the center of its mass [7]. Polymer molecules in a solution, depending on the concentration, can preferentially link to other polymer molecule [8]. The polymer will also concurrently attach to oxide powder particle surface with its positive part of the chain. That is in polyvinyl alcohol hydrogen bond positioned all along the polymer chain. Oxide powder particle surface is sometimes charged due to hydroxylation and reacts with polymer through hydrogen bond formation [9]. The concurrent processes, agglomeration of the polymer and attachment to the oxide particle surface are both kinetically hardly traceable processes. The occupation of the overall powder`s particle surface with folded polymer chains, as well as the surface that is occupied with one polymer molecule, radius of gyration, are important properties described by different parameters and characterization techniques. These oxide-polymer processes are frequently encountered as a topic of the numerous investigations [10].

The processes that govern polymer segregation over the compact volume often lead to an uneven distribution of the polymer and thus intense burnout during sintering invoking unavoidable deterioration of the sintered specimen [11,12]. Nevertheless, most often when resolving these problems, varying the simplest parameter – binder amount is helpful. Usually, according to numerous literature data, it is found that polymer mass percent can't be more than 3 wt% [13,14]. By using appropriate small percentage of the binder, it is expected that the polymer will attach maximally on the ceramic`s powder surface, but at the same time it should enable avoidance of the mutual connections between polymer chains and their segregation.

If the poly-vinyl alcohol is taken as a binder, then compact is also prone to swelling process since PVA adsorbs available $H_2O$, usually present as humidity [15,16]. To prevent the $H_2O$ incorporation, as well to improve mechanical properties of the compact, the small amount of the poly-ethylene glycol can be added to the main PVA polymer as a plasticizer [17]. Expectation is that side chains of PVA will graft on PEG backbone resulting in a graft-copolymer [18] (Fig. 1).

This work has an intention to characterize the changes induced by the introduction of the PVA and PVA-PEG polymers as a compaction binder on the compaction of the oxide powders mixture ZnO, $Mn_2O_3$ ($MnCO_3$) and $Fe_2O_3$.

Amount of the polymer added to the oxide powder mixtures was varied also. Characterization techniques have been selected as oriented on the observation of the fundamental interaction between oxide powder particle surface and polymer. Besides these, influences on compaction and sintering synthesis routes induced by binder were also

observed. Processing techniques as - handling tools easiness during compaction, as well as dimensional changes during sintering due to the polymer burnout process, were discussed.

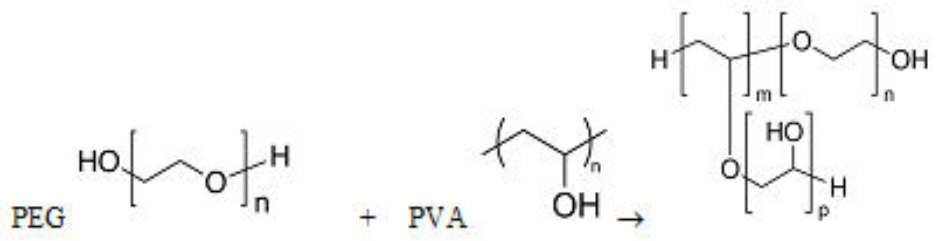


**Fig. 1.** Formation of the graft-copolymer from polyvinyl alcohol (PVA) and polyethylene glycol (PEG).

## 2. Materials and Experimental Procedures

A mixture of ZnO and $Fe_2O_3$ powders (ZnO 205532 Aldrich, $Fe_2O_3$ Aldrich 310050) was mixed with $Mn_2O_3$ or $MnCO_3$ ( $Mn_2O_3$ Aldrich 377457, $MnCO_3$ Aldrich 377449), and the resulting powder mixtures were hereinafter referred to as MZF or MCZF, respectively.

The ratio of the oxides is chosen as 21wt% $Mn_2O_3$, 13wt% ZnO, and 66wt% $Fe_2O_3$, for MZF and 28wt% $MnCO_3$, 12wt% ZnO and 60wt% $Fe_2O_3$ for MCZF to follow already used Mn-Zn ferrite stoichiometry $Mn_{0.63}Zn_{0.37}Fe_2O_4$ that we have investigated before [19]. In the following text, inorganic powders are referred as an oxide powders although the carbonates are present, and when the influence of the oxide - carbonate difference is discussed it will be particularly emphasized. All mixed powders were homogenized in a rotary mill for 20 minutes, using $ZrO_2$ balls (1 mm diameter) with 80g of balls + 20g of powder = 4:1 ball-to-powder weight ratio. Polymers used were PVA (Mw 89,000 – 98,000; 99%+ hydrolyzed, Aldrich 341584), and two different PEG: 8000 Aldrich P2139 and Fortrans Macrogol 4000. Different PEG starting polymers are used since we wanted to examine difference in PEG polymer chain molecular weight influence. The aqueous suspension of oxide powders mixture was formed by pouring a weighted amount of powder into the beaker with water, after which the ultrasonic deagglomeration in a water bath was performed. Water solutions of 8% PVA and 4% PEG were made separately with the purpose of addition to powders suspension in an appropriate amount for forming desired polymer to oxide powders dispersions ratio. These ratios were 20%wt PVA, 20%wt PVA + 6%wt PEG and 2%wt PVA + 0.6%wt PEG. Percentages are referring to mass percentage ratio of the polymer to oxide powder. Water dispersions were formed, giving polymer to oxide before mentioned ratios. These water dispersions were ultrasonically homogenized and then evaporated at 60ºC during 24 hours until water dried completely and oxide powders with wanted amount of polymer were obtained. In order to differentiate the potential function of the polymer, the designations P (polymer) for composite for high polymer content (20%PVA, and 20%PVA +6%PEG) and B (binder) for low polymer content were introduced (2%wt PVA + 0.6%PEG) in labeling. The solutions containing only polymers with PVA: PEG = 20:6 ratio were as well formed. By solution drying of PVA : PEG = 20:6 ratio, until all water evaporated, solid plastic specimen of just polymers was obtained, designated as PVA + PEG A.

The specimen`s labeling of the powder mixtures, obtained polymers without oxide powders, and also oxide powders with polymers are as denoted in Table I.

**Tab. I.** Annotation of the specimens.

| | |
|---|---|
| **1MZF** | 21wt%$Mn_2O_3$, 13wt%ZnO, 66wt%$Fe_2O_3$, homogenized mixture. |
| **2MCZF** | 28wt%$MnCO_3$ 12wt%ZnO, 60wt%$Fe_2O_3$ homogenized mixture. |
| **3MZF-P_PVA20** | MZF powder mixture with 20% of PVA. |
| **4MZF-B_PVA2+PEG06** | MZF powder mixture with PVA2 % and 0.6% PEG. |
| **5MCZF-B_PVA2+PEG06** | MCZF powder mixture with PVA 2% and 0.6% PEG. |
| **6MZF-P_PVA20+PEG6** | MZF powder mixture with PVA 20% and 6% PEG. |
| **7PVA+PEG-A_20:6** | PVA:PEG = 20:6 ratio, just polymers, obtained by drying. |
| **8PEG-A** | Aldrich P2139 starting polymer in a solid state |
| **9PEG-M** | Fortrans Makrogol 4000 starting polymer in a solid state |
| **10PVA** | Aldrich 341584, starting polymer in a solid state |

Drying at 60ºC for 24 hours has led to dried residue for all specimens, so called "cake" at the beaker bottom. Low drying temperature ensures avoidance of glass transition temperature estimated at 83°C to 95.9ºC using DSC analysis of PVA. Drying is followed by scrubbing the dried precipitate from the beaker. Precipitates were homogenized by milling in the mortar grinder Pulverisette 2 Fritsch for 30 minutes.

Thermal DSC characterization was carried out with Setaram DSC 131 evo model at heating rate ($\beta$) 10ºC/min in flowing nitrogen atmosphere. Thermo gravimetric and differential thermal analysis TG/DTA was recorded for polyvinyl alcohol polymer on Setaram SETSYS Evolution TGA-DTA/DSC device, $\beta$=10ºC/min in nitrogen atmosphere. Infrared spectroscopy measurements were performed at FTIR Nicolet 6700 equipped with an attenuated total reflection (ATR) accessory (single-bounce diamond crystal Smart Orbit micro-ATR). Transmission electron microscopy TEM was recorded at JEOL JEM 1400 plus microscope. Dilatometry was recorded on Bahr 802 s dilatometer at 10ºC/min heating rate up to 400ºC.

Compaction was conducted on a hydraulic press RING, P-14, VEB Thuringer, in a 8 mm tool diameter consisting of a die and cylinder, with double sided uniaxial compaction technique. Compact shapes were cylindrical, with mass of 0.5 g. Heating of the compacted specimen was performed on the dilatometric device at 10ºC/min heating rate, up to 575°C.

## 3. Results and Discussion

Thermal behavior of the polyvinyl alcohol is presented as TGA/DTA recording at Fig. 2. Mass loss of 5% is subscribed to dehydration, removing of water, and thermal degradation of large chains into smaller fragments extensively at 133ºC up to 200°C. Obtained DTA thermal event starting at 83.5ºC up to 95.9ºC is assigned as a glass transition temperature, *T*g, value. Than follows, without mass loss at TG curve, on DTA curve at 221.8ºC transition from solid to liquid, point where each polymer chain molecule exists alone. After that DTA signal at 266.1°C comes from decomposition of side chains, and at 289.6ºC peak at DTA diagram with an intensive mass loss is originating from oxidation combustion of the main chain polymer [20]. Mass loss diagram from 266.1ºC refers to degradation of PVA. Namely adjacent acetyl and hydroxyl groups will be eliminated as acetic acid and water and

result in conjugated double bonds and unsaturated carbonyl groups, which have higher bond energies than C-OH, and would enhance the stability of PVA and result in five and six-member rings giving rise to the temperature during further heating [21].

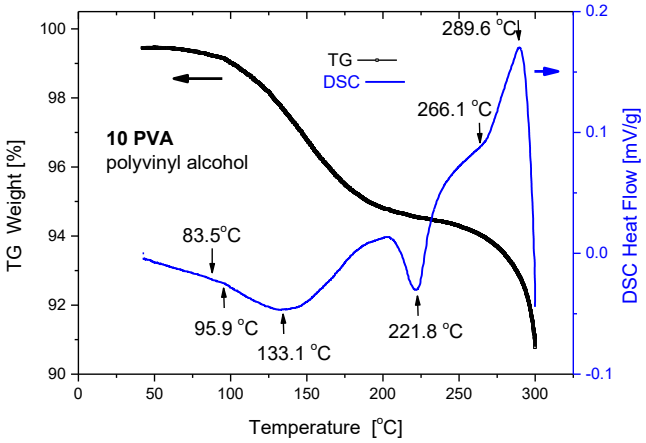


**Fig. 2.** TG/DTA diagram of PVA - Poly vinyl alcohol, **10 PVA.**

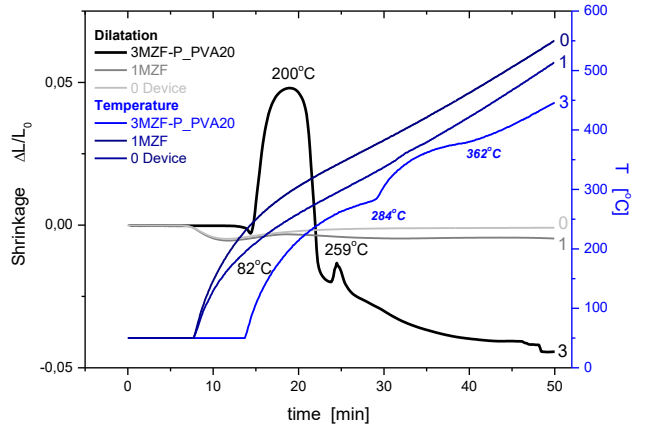


**Fig.3.** Relative shrinkage and temperature profiles of the powder compacts with PVA, **3MZF-P_PVA20**, without binder (dry) **1 MZF**, and **0 Device** system shrinkage with empty dilatometer (blank).

Dilatation measurements presented in Fig. 3. were recorded for the oxide compacts (1MZF), the oxide compacts with PVA (**3MZF-P_PVA20**), and dilatometer device system without specimen (0 Device). Binder burnout is an intensive event regarding dimensional changes. It represents the sample deterioration during the burn out of the polymer. These changes can overlap the events originating from metal oxide shrinkage in the observed temperature region [11]. The point of polymer glass transition *T*g, recorded in interval 83.5ºC up to 95.9ºC at Fig. 2 is recognizable as minima on the 82°C, but can be regarded as overlapped with event with the peak at 200ºC. The 200ºC peak is swelling due to softening of the polymer. It originates from before mentioned adjacent acetyl and hydroxyl groups elimination as acetic acid and water. These products lead to intensive swelling up to 200°C. Next peak, lower in intensity at 259°C, is subscribed to the acetyl group elimination as carboxyl acid and unsaturated aldehydes. It can be regarded as same in origin with 266.1°C shoulder at DSC curve on Fig. 2, where the difference is subscribed to the fact that dilatometric measurements are performed on the oxide powder with PVA. At 284°C

thermocouple of the dilatometer device is recording deviation from usual temperature schedule as a temperature increase, what is evidence for the burnout process although shrinkage is not interrupted. TG/DSC, at Fig. 2, diagram with 289°C can be taken as more prompt temperature of the onset of the same event.

The blending of the PVA with PEG forms a graft copolymer. Due to the formation of the graft – copolymer, expectation is that characteristic temperatures will differ for PVA - PEG combination. It can, as well, lead to different conformations of the cross linked polymer blend made of two polymer chains.

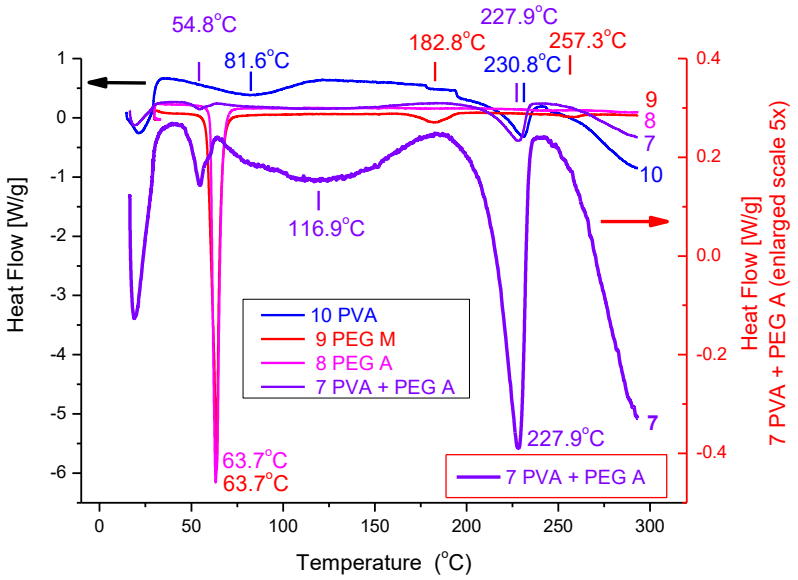


**Fig. 4.** DSC diagram of the samples **7PVA+PEG-A_20:6**, and **10PVA**, **9PEG-M**, **8PEG-A**, as well **7PVA+PEG-A_20:6**, 5 times enlarged scale at the right side axis.

At Fig. 4, **7PVA+PEG-A_20:6** specimen's thermogram represents the combination of the polymers shown on the right, as well on the left axis. We can see that broad peak at 116.9°C emerges as new one compared to both pure polymers PVA or PEG. The **7PVA+PEG-A_20:6** specimen at DSC diagram is indicating that graft copolymer is formed, and also that all PEG content is consumed by PVA which is nominally in surplus. PVA on DSC diagram, Fig. 4, gives characteristic temperatures at 81.6°C and 230.8°C. First peak should be assigned to temperature of the glass transition *T*g of PVA, and second one to melting of the PVA. The values are in accordance with, Fig. 2, thermal dilatation presented before. Pristine PEG diagram, **9PEG-M** and **8PEG-A**, both have endo minima very sharply outlined at 63.7°C, and it is same for both specimens. The absence of the PEG characteristic peak in the **7PVA+PEG-A_20:6** can be possibly declared as existing at 54.8°C, but with the intensity drastically lowered. Peak present for the PVA at 230.8°C, when PEG is added, is somewhat shifted to lower temperatures, namely to 227.9°C. Also, the difference between pharmaceutical PEG M and pure PEG A is in two peaks existing at **9PEG-M**, 182.8°C and 257.3°C, due to the additives for medication purpose.

At Fig. 6. DSC diagrams for the samples of oxide particles tightened to the polymer, as well as the samples of pristine oxide powders in the range up to 300°C are presented. Water suspension of oxides particles in a diluted polymer is treated by the evaporation of the water at the temperature below *T*g of the PVA. Graft-copolymer tightened to the powder particles has been obtained, what is schematically presented at Fig.5. In such a manner by comparing polymer behavior presented on Fig. 4. and polymer attached to oxide power particle surface,

oxide particles without polymer, on Fig. 6. difference that is indicating interaction of polymer – oxide particle, can be distinguished.

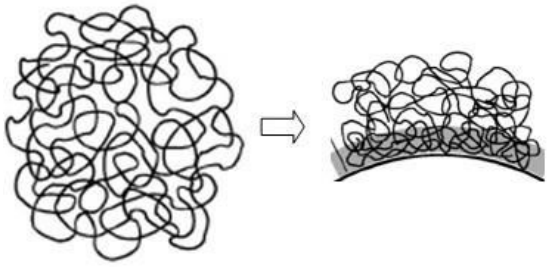

**Fig. 5**. Schematic representation of the non adsorbed polymer and attachment on the surface of the powder particle.

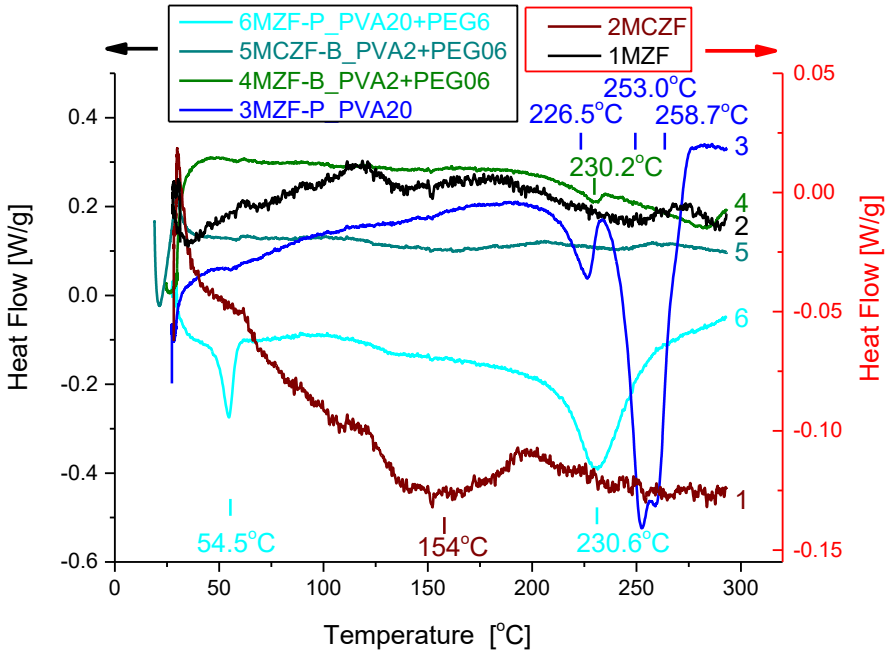


**Fig. 6.** DSC diagram of the samples of oxide powders, **1MZF**, **2MCZF** right axis enlarged scale, and oxide powders with polymers **3MZF-P_PVA20**, **4MZF-B_PVA2+PEG06**, **5MCZF-B_PVA2+PEG06**, **6MZF-P_PVA20+PEG6,** left axis.

If we observe interactions between oxide powders and polymers it should be regarded as compared to a difference with DSC curves of pristine oxide powders mixture **1MZF**, **2MCZF**, Fig. 6, which are assigned to right axes with red scale due to different magnitude order. Difference between, **1MZF** and **2MCZF**, is that the first one does not contain carbonate. Adsorbed water on the specimen with carbonates desorbs with a temperature rise what is recorded as a low extended peak of water desorption from carbonates at 154°C [23,24].

In the sample **6MZF-P_PVA20+PEG6** ten times higher weight percent amount of 20% PVA+ 6% PEG of graft polymer PVA-PEG declares peak for PVA at 230.6°C and for PEG at 54.5°C as characteristic graft PVA-PEG polymer peaks. Concentrations of 2% PVA+0.6% PEG in the polymers blend, samples **4MZF-B_PVA2+PEG06** and **5MCZF-B_PVA2+PEG06**, on DSC diagram unfortunately, are neither representation of the polymer

behavior nor the interaction of the polymer with oxide powders due to their low content of polymer (Fig.6). For the sample **4MZF-B_PVA2+PEG06**, PVA peak is positioned at 230.3°C and detectable, but for the sample **5MCZF-B_PVA2+PEG06**, possible reaction between carbonates and polymer leads to a broaden peak in a wide temperature domain and absence of the PVA peak.

On DTA signal of sample **3MZF-P_PVA20** (MZF oxide and high PVA content), the peak for PVA 226.5°C is present, as well as two PVA peaks 253.0°C and 258.7°C that are absent in the PVA-PEG polymer alone (**7PVA+PEG-A_20:6**, on the Fig. 4). The absence of the two PVA peaks, namely 253.0°C and 258.7°C, at **3MZF-P_PVA20**, comparing with **6MZF-P_PVA20+PEG6** diagram, leads to a conclusion that graft copolymer is formed and detected at DTA diagrams only if the concentration of the polymer is high enough (Fig. 6). Infrared spectroscopy is a very useful technique for understanding interaction between organic coating and inorganic particles since it can compare optical properties of coated and pristine oxide particles at the same time. Comparing polymer spectra (Fig. 7), without oxide particles, polymer mixture **7PVA+PEG-A_20:6** and spectra of starting two polymers **8PEG-A** and **10PVA,** combined polymer consists of bands already present in the individual spectra of the polymers, with the exception of the 1739 $cm^{-1}$ band that does not exist in an individual polymer spectra. Existence of this band indicates the formation of the bond between two polymer chains. In such a manner observations presented within a thermal characterization approach were affirmed. Namely, polyvinyl alcohol-polyethylene glycol PVA–PEG graft copolymer is formed. Polyvinyl alcohol (PVA)-polyethylene glycol (PEG) graft copolymer is a graft copolymer of ethylene glycol and vinyl alcohol consisting of approximately 75% vinyl alcohol units and 25% ethylene glycol units [25]. Also indication of the changes in the PVA-PEG graft copolymer spectra from the single polymer is the shift of the bands. PEG band declared at 2881 $cm^{-1}$ is shifted from 2878 $cm^{-1}$ for pure PEG to 2887 $cm^{-1}$ PEG –PVA, hipsochromatic - blue shift. PVA stretching OH band from declared PVA 3303 $cm^{-1}$ is shifted from 3273 $cm^{-1}$ to 3298 $cm^{-1}$ in PEG-PVA.

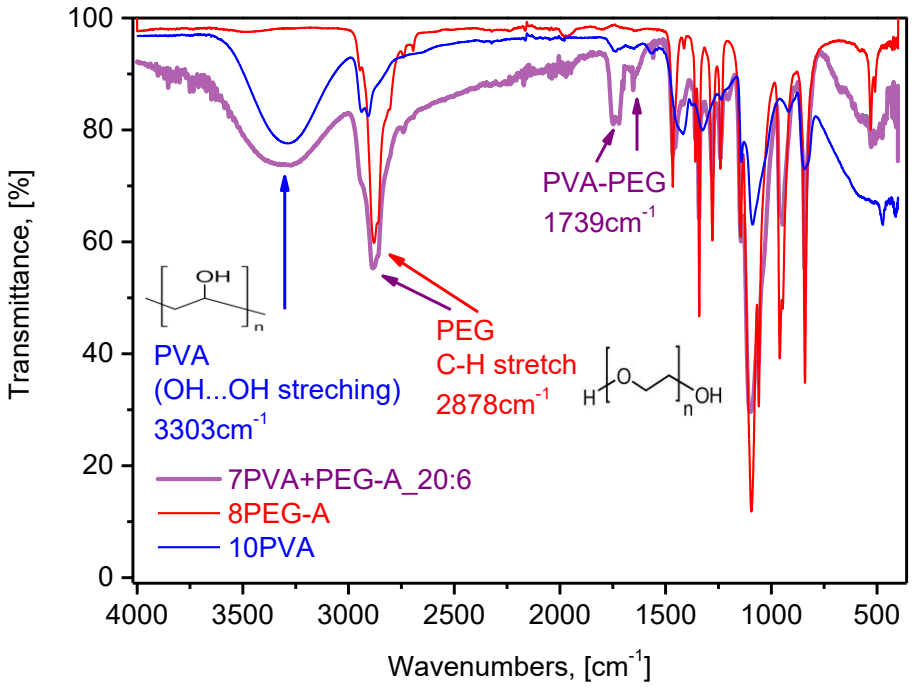


**Fig. 7.** FTIR spectra of the pristine PVA polymer **10PVA**, pristine PEG polymer **8PEG-A** polymer, and formed **7PVA+PEG-A_20:6**, all obtained from water solution by evaporation.

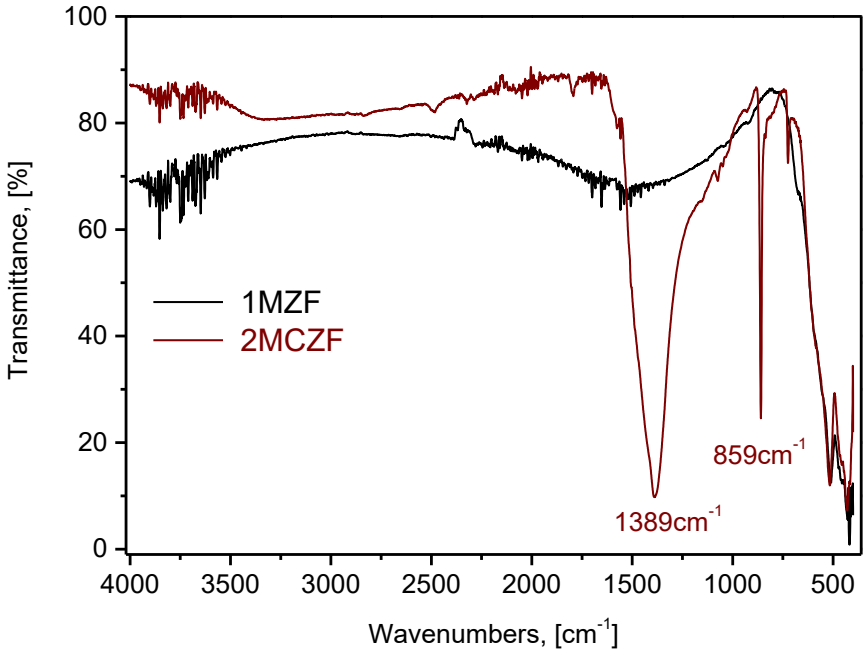


**Fig. 8.** Infrared spectra of the starting mixtures of oxide powders, **1MZF**, **2MCZF**.

If we observe FTIR spectra of the pristine oxide and carbonate powder mixtures without polymer, Fig. 8, it is worth emphasizing that the difference is band 1389 $cm^{-1}$ and 859 $cm^{-1}$ which belong to the carbonate group in a **2MCZF** and they do not exist for $Mn_2O_3$ containing mixture, **1MZF**. Therefore, it is more convenient to observe the inorganic-polymer interaction spectra using oxide powders, rather than carbonates [26].

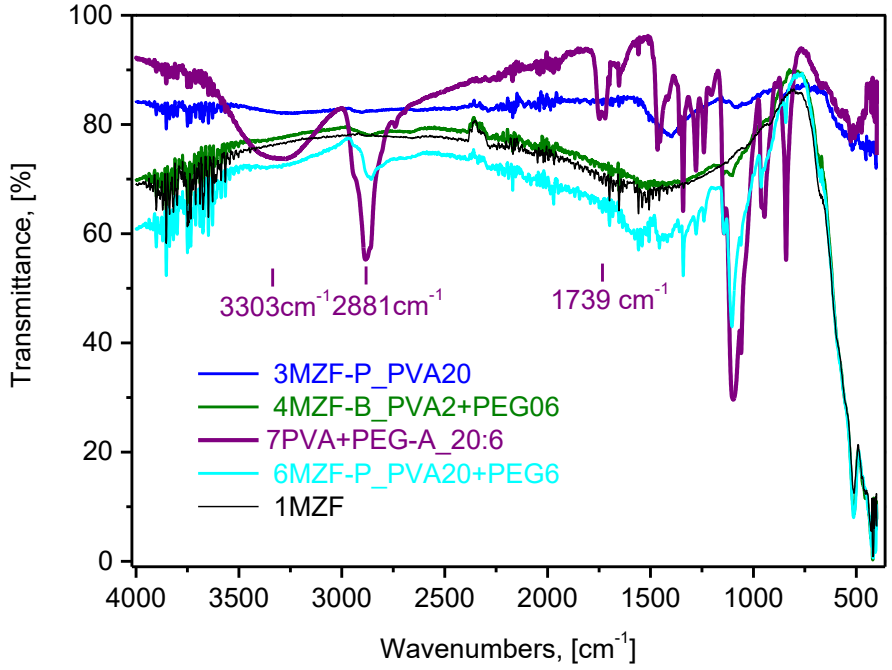


**Fig. 9.** FTIR spectra of the specimens: **1MZF**, **3MZF-P_PVA20**, **4MZF-B_PVA2+PEG06**, **6MZF-P_PVA20+PEG6**, **7PVA+PEG-A_20:6**.

FTIR spectra of the polymer mixture attached to the oxide particles, **3MZF-P_PVA20**, **4MZF-B_PVA2+PEG06**, **6MZF-P_PVA20+PEG6**, compared to polymer mixture alone **7PVA+PEG-A_20:6**, and oxide powder alone **1MZF**, FTIR spectra, are all presented on Fig. 9. Band at 2881 $cm^{-1}$ PEG A is present in all concentrations of polymer mixtures regardless of the PEG concentration present. Also 1739 $cm^{-1}$ band that we have subscribed to graft polymer is present but detectable only for the specimen **6MZF-P_PVA20+PEG6**. That means that graft polymer is present and detectable in higher concentrations. Specimen with PVA alone with 20% PVA (**3MZF-P_PVA20**) does not indicate existence of the before mentioned band. Band 2881$cm^{-1}$ of the PEG chain, **7PVA+PEG-A_20:6** at 2878 $cm^{-1}$, in the polymer mixture attached to the oxide surface existed in all observed specimens, (**4MZF-B_PVA2+PEG06**, **6MZF-P_PVA20+PEG6)**. The band at 3303 $cm^{-1}$ noted at the Fig. 7, belongs to PVA–OH stretching interaction, in the presence of oxide power particles surface has lowered intensively and even disappeared (**3MZF-P_PVA20, 4MZF-B_PVA2+PEG06**, **6MZF-P_PVA20+PEG6**) indicating the connection of the polymer and oxide particles surface.

If the specimen is properly prepared, transmission electron microscopy can show the difference between oxide particles and the polymer binder in the compact. Distance difference between oxide particles is formed by pinched adsorbed polymer layer. TEM micrograph at Fig. 10 was performed at a specimen **4MZF-B_PVA2+PEG06** with lower content of the polymers that suites binder. Particles are detectable and the distance between them should indicate the thickness of the adsorbed layer, but unfortunately it is not estimable. Agglomeration is present, with agglomerate dimensions around micrometer, what leads to the conclusion that nano dimensional oxide powder intensively agglomerates in the polymer suspension. Also this means that nano powder particles were not separated well, but rather stayed agglomerated, regardless of the fact that ultrasound deagglomeration has been performed.

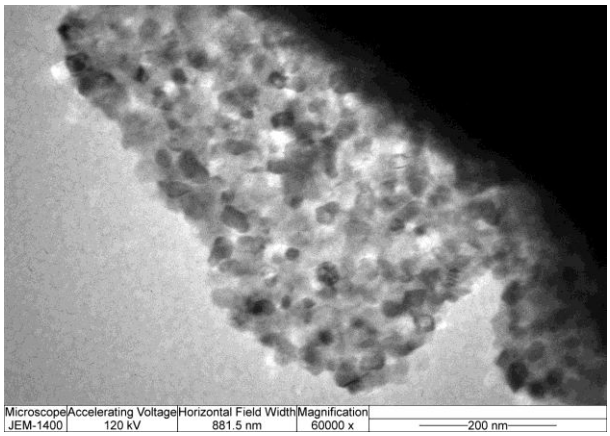


**Fig. 10.** TEM micrograph of the **4MZF-B_PVA2+PEG06**.

Second picture with the same magnification, Fig. 11, exhibits specimens with higher concentration of polymer, **6MZF-P_PVA20+PEG6**. Large domains of the polymer and individual powder particles are found completely separated. Nano particles in the water solution are hardly stabilized [27] so it seems that the intensive agglomeration presented on Fig. 10 is avoided in the polymer with higher concentration due to high viscosity of the polymer solution. Particles that were found loose free in the suspension are trapped individually in the polymer surrounding during evaporation. Although, the presented mutually attached nano particles on the highest magnification, Fig. 12, for the same specimen **6MZF-P_PVA20+PEG6**, are showing existence of small agglomerates that are consisted of only few

closely attached nano particles with no space between them indicating in such a manner extremely thin polymer layer.

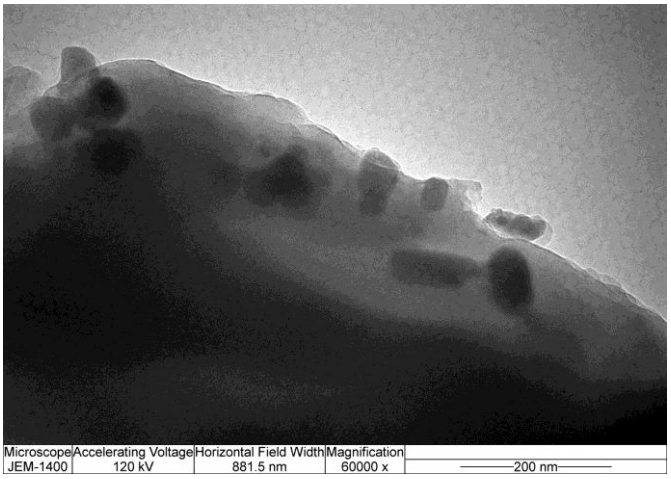


**Fig. 11.** TEM micrograph of the **6MZF-P_PVA20+PEG6**.

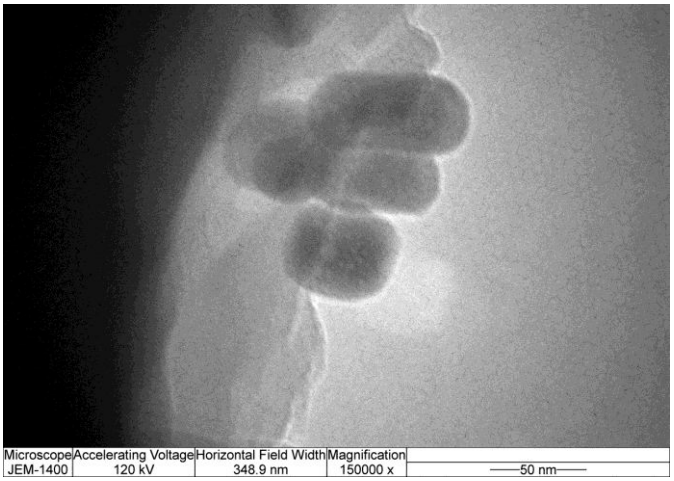


**Fig. 12.** TEM micrograph of the **6MZF-P_PVA20+PEG6**.

The intention was to separate powder particles in the suspension of the polymer solution by ultrasonic agitation. Afterwards next step, evaporation of water, regardless of the evaporation kinetics, should be independent of agglomeration. However, if the concentration of the polymer in suspension is higher, the viscosity of the suspension also rises and the agglomeration is hindered since the mobility of the distributed powder particles is lost. Here presented synthesis route for polymer and oxide particle attachment implies the concurrent processes. Namely, during evaporation of water, polymer gelates [28] and as well concurrently adsorbs on the oxide powder surface. In our case these competing reactions are probably hindered with prompt powder agglomeration and graft copolymer formation that is afterward fixing agglomerates positions in polymer matrix during drying. Agglomeration of the oxide particles and simultaneous formation of the gelated PVA – PEG graft copolymer domains without oxide powders incorporated, leads to formation of a non uniform material. As it is presented from the micrographs, this powder-polymer segregation is not significantly suppressed with polymer concentration change and ultrasonic treatment that precedes the

suspension formation. The observed kinetic problem can be probably avoided with the use of a spray drier device [29-31].

All of the before mentioned reasons are influencing the compaction ability. It was noted during compaction of the nano powders without binder that the nano particles agglomerate and interfere with microscopic dimension of the tool tolerance gap. Addition of the PVA has solved the problem since PVA as a binder did not cause stacking problems. Used alone, PVA enables friction reduction due to water absorption from atmospheric humidity. It is worth emphasizing that compaction is hindered for the nano oxide powder binded with plasticized PVA-PEG graft polymer. Namely, formed agglomerates connected with PVA-PEG binder, often stuck in the tolerance gap of the compaction tools, causing friction that stops regular movement of the tool. These agglomerates are expected to be mechanically stronger than one without the binder. In the PVA-PEG as a binder, blocking of the tool is attributed to the stiffening caused by the graft polymer. Introducing stearic acid as a lubricant was found ineffective in both situations mentioned before [32].

## 4. Conclusion

PVA polymer and PVA-PEG graft polymer were deposited on metal oxide nano particles powder mixture. Influence on polymer chains was observed with FTIR, DTA and TEM characterization techniques. We have indicated with infrared spectra that after drying graft polymer is formed from PVA-PEG. Formed graft polymer during drying interacted with oxide powder. The thermal behavior of the powders with polymers supports the fact that oxide powders are interacting with the polymer showing characteristic temperature shift on the DTA diagram. TEM micrographs are indicating that the micrometric dimensions of the agglomerates formed of nano powder particles are separated from pure polymer regions. That is in collision with the even binder distribution presumption and compaction utilization itself. Also the plasticizing PVA with PEG adding leads to a tool stacking due to rearranging disability of nano powder agglomerates in the gap of compaction tool.

## Acknowledgments

This work was supported by the Ministry for Science, Education and Technological Development of the Republic of Serbia, Projects OI172057 and III45014 and III 45001. Funds for the realization of this work are provided by the Ministry of Education, Science and Technological Development of the Republic of Serbia, Agreement on realization and financing of scientific research work of the Institute of Technical Sciences of SASA in 2022 for Nebojša Labus (Record number: 451-03-68/2022-14/ 200175). Also the important help was a personal communication with Prof. Milenko Plavšić and Dr Miodrag Zdujić. Authors would like to express thank for performed thermal characterization to Dr Smilja Marković at TGA/DTA device ITS SASA laboratory.

## 5. References

1. M. Abdel-Ghani, J. G. Petrie, J. P. K. Seville, R. Clift , M. J. Adams, Mechanical properties of cohesive particulate solids, *Powder Technology,* 65 (1991) 113-123.
2. Keizo Uematsu, Processing defects in ceramic powders and powder compacts, *Advanced Powder Technology,* 25 (2014) 154-162,

3. N. Labus, J. Krstić, S. Marković, D. Vasiljević-Radović, M V. Nikolić, V. Pavlović, $ZnTiO_3$ Ceramic Nanopowder Microstructure Changes During Compaction, *Science of Sintering,* 45 (2013) 209-221.
4. L. Xu, R. Helstroom, O.J. Scott, A.J. Chambers, Fracture Characteristics of Powder Compacts, *Powder Technology,* 83 (1995) 193-199.
5. P. Druska and U. Steinike, V. Sepelak, Surface Structure of Mechanically Activated and of Mechanosynthesized Zinc Ferrite, *Journal of Solid State Chemistry,* 146, 1 (1999) 13-21.
6. Asep Bayu Dani Nandiyanto, Kikuo Okuyama, Progress in developing spray-drying methods for the production of controlled morphology particles: From the nanometer to submicrometer size ranges, *Advanced Powder Technology*, 22 (2011) 1-19,
7. A. Ravve, Principles of Polymer Chemistry, Third Edition, Springer, 2012, DOI 10.1007/978-1-4614-2212-9
8. Leonid K. Filippov, Cesar A. Silebi, and Mohamed S. El-Aasser, Kinetics of Adsorption of Water-Soluble Associative Polymer on a Planar Titanium Dioxide Surface, *Langmuir*, 11(1995) 872-879.
9. Tse-Hsing Ho, Shinn-Jen Chang, Chia-Chen Li, Effect of surface hydroxyl groups on the dispersion of ceramic powders, *Materials Chemistry and Physics,* 172 (2016) 1-5.
10. A. Doroszkowski, R. Lambourne, A Viscometric Technique for Determing the Layer Thickness of Polymer Adsorbed on Titanium Dioxide, *Journal of Colloid and Interface Science,* 26 (1968) 214-221,
11. R. Mauczok, V.T. Zaspalis, Binder burnout-material-process interaction during sintering of MnZn-ferrites, Journal of the European Ceramic Society, 20 (2000) 2121-2127.
12. Samir Baklouti, Jamel Bouaziz, Thiery Chartier, Jean-Francois Baumard, Binder burn out and evolution of the mechanical strength of dry-pressed cermics containing poly (vinyl alcohol), *Journal of the European Ceramic Society,* 21 (2001) 1087-1092.
13. David C. C. Lam, Effects of Binder and Compaction Pressure on Strength and Fracture Origins in Bodies Pressed from Granules, *Journal of the Ceramic Society of Japan*, 102 [11] (1994) 1010-1015.
14. Philomina Ekka, Effect of binders and plasticisers on alumina processing, A Thesis Submitted In Partial Fulfillment of the Requirement For the degree of Bachelor of Technology, To the Department of Ceramic Engineering, National Institute of technology Rourkela, Odisha, India, June 2011.
15. Robert D. Carneim, Gary L. Messing, Response of granular powders to uniaxial loading and unloading, *Powder Technology,* 115 (2001) 131-138,
16. Yutaka Saito, Junichi Nyumura, Yao Zhang, Satoshi Tanaka, Nozomu Uchida, Keizo Uematsu, Kinetics of property change associated with atmospheric humidity changes in alumina powder granules with PVA binder, *Journal of the European Ceramic Society,* 22 (2002) 2835-2840.
17. C. W. Nies, G. L. Messing, Effect of Glass-Transition Temperature of Polyethylene Glycol-Plasticized Polyvinyl Alcohol on Granule Compaction*, J. Am. Ceram. Soc,* 67, [4] (1984) 301-304.
18. Franziska F. Heuschmid, Paul Schuster, Polyethylene glycol–polyvinyl alcohol grafted copolymer: Study of the bioavailability after oral administration to rats, *Food and Chemical Toxicology,* 51 (2013) S3–S6.
19. Nebojša Labus, Zorka Vasiljević, Obrad Aleksić, Miloljub Luković, Smilja Marković, Vladimir Pavlović, Slavko Mentus, Maria Vesna Nikolić, Characterisation of $Mn_{0.63}Zn_{0.37}Fe_2O_4$ Powders After Intensive Milling and Subsequent Thermal Treatment, *Science of Sintering,* 49 (2017) 455-467.

20. K. Naveen Kumar, R. Padma, Bright green emission from f-MWCNT embedded co-doped $Bi^{3+}$+$Tb^{3+}$:polyvinyl alcohol polymer nanocomposites for photonic applications, *The Royal Society of Chemistry.,* 7 (2017) 15084-15095.
21. Haigang Yang , Shoubin Xu , Long Jiang & Yi Dan, Thermal Decomposition Behavior of Poly (Vinyl Alcohol) with Different Hydroxyl Content, *Journal of Macromolecular Science, Part B: Physics*, 51:3 (2012) 464-480
22. Jyongsik Jang, Dong Kweon Lee, Plasticizer effect on the melting and crystallization behavior of polyvinyl alcohol, *Polymer*, 44 (2003) 8139-8146,
23. L. Biernacky, S. Pokrzywincky, The thermal decomposition of Manganese Carbonate Thermograviemtry and Exoemission of Electrons, *Journal of Thermal analysis and Calorimetry,* vol.55 (1999) 227-232.
24. Yang Liua, Pengyi Zhangb, Jingjing Zhana , Lifen Liu, Heat treatment of $MnCO_3$: An easy way to obtain efficient and stable $MnO_2$ for humid $O_3$ decomposition, *Applied Surface Science*, 463 (2019) 374-385.
25. S. M. F. Jeurissen, et al. "Polyvinyl alcohol (PVA)–polyethylene glycol (PEG) graft copolymer." Safety evaluation of certain food additives and contaminants. World Health Organization, 2016, 88-106.
26. P. Vishnu Vardhan, C. Jothilakshmi, U. Kamachi Mudali and S. Devaraj, The Effect of Carbonate Precursors on the Capacitance Properties of MnCO3, *Materials Today: Proceedings,* 4 (2017) 12407-12415.
27. C. P. Tso, Stability of metal oxide nanoparticles in aqueous Solutions, *Water Science & Technology-WST*, 61,1, 2010.
28. E. Bormashenko et al., Self-assembly in evaporated polymer solutions: Influence of the solution concentration, *Journal of Colloid and Interface Science,* 297 (2006) 534-540.
29. Agnese Stunda-Zujeva, Zilgma Irbe, Liga Berzina-Cimdina, Controlling the morphology of ceramic and composite powders obtained via spray drying – A review, *Ceramics International,* 43 (2017) 11543-11551.
30. Padmaja Parameswaran Nampi, Shoichi Kume, The effect of polyvinyl alcohol as a binder and stearic acid as an internal lubricant in the formation, and subsequent sintering of spray-dried alumina, *Ceramics International,* 37 (2011) 3445-3450.
31. Asep Bayu Dani Nandiyanto, Kikuo Okuyama, Progress in developing spray-drying methods for the production of controlled morphology particles: From the nanometer to submicrometer size ranges, *Advanced Powder Technology*, 22 (2011) 1-19.
32. A. R. Baichwal, L. L. Augsburger, Variations in the friction coefficients of tablet lubricants and relationship to their physicochemical properties, *Journal of Pharmacy and Pharmacology*, Volume 40, Issue 8, August 1988, Pages 569-571.

***Сажезак:*** *Смеша прахова састављена од ZnO, $Mn_2O_3$ ($MnCO_3$) и $Fe_2O_3$ комбинације прахова је показивала ламинацију током пресовања. Поливинил алкохол (PVA) и комбинација PVA са полиетилен гликолом (PEG) који је додат као пластификатор, су уведени као полимерно везиво за пресовање оксидних прахова. Везиво је уведено тако што је формирана суспензија смеше различитих оксида прахова у полимерном раствору. Концентрације полимера и састави су варирани. Уклањањем растварача добијени су нови материјали који се састоје од честица оксида повезаних полимерима. Ови хибридни материјали окарактерисани су методама ометене тоталне рефлексије фурије трансформисане инфрацрвене спектроскопије (ATR-FTIR) као и диференцијалне термичке анализе (DTA). Микроструктура је посматрана трансмисоном електронском микроскопијом (TEM). Оксид-полимер материјали су пресовани на притиску од 200 MPa и ширење испреска током грејања је праћено у*

*температурском опсегу од собне до 550°C употребом дилатометра. Нађено је да PVA формира графт полимер са PEG и да постоји специфична интеракција полимера са површином честица оксида.*
***Кључне речи**: оксидни на-прах, компактирање, термална својства, PVA везиво.*